

# Development of a debris index

Francesca Letizia, Camilla Colombo, Hugh G. Lewis and Holger Krag

**Abstract** Environmental indices for space objects have been proposed to identify good candidates for active debris removal missions and to deal with the licensing process of space objects before their launch. A way to rank the environmental impact of spacecraft may be based on the assessment of how their fragmentations would affect operational satellites. In particular, the effect of a breakup can be measured by the resulting collision probability for a set of target spacecraft. A grid in semi-major axis, inclination, and mass is used to define possible initial conditions of the breakup. Once the value of the index is known for any point in the grid, a simple interpolation can be used to compute the value of the index for any object. The current work aims to extend a previous formulation, which focussed only on the effect of collisions, by including also the effect of explosions and considering the likelihood of these fragmentations.

## 1 Introduction

The space around the Earth is populated by an increasing number of objects and most of them are not operational ones. According to the European Space Agency

---

Francesca Letizia  
University of Southampton, University Road, SO17 1BJ, Southampton, United Kingdom, e-mail: [f.letizia@soton.ac.uk](mailto:f.letizia@soton.ac.uk)

Camilla Colombo  
Politecnico di Milano, Via La Masa 34, 20156 Milan, Italy, e-mail: [camilla.colombo@polimi.it](mailto:camilla.colombo@polimi.it)

Hugh G. Lewis  
University of Southampton, University Road, SO17 1BJ, Southampton, United Kingdom, e-mail: [h.g.lewis@soton.ac.uk](mailto:h.g.lewis@soton.ac.uk)

Holger Krag  
European Space Agency, ESOC, Darmstadt, 64293, Germany e-mail: [Holger.Krag@esa.int](mailto:Holger.Krag@esa.int)

(ESA)<sup>1</sup>, out of the 23000 catalogued objects, only around 1000 are operational satellites whereas the rest is composed by spent satellites, mission related objects and, mainly, fragments produced by explosions and collisions.

The analysis of the evolution of these numbers over time has suggested the adoption of measures to limit the growth of the debris population such as the passivation of rocket bodies (to limit the risk of explosions) and the definition of protected orbital regions that should be left clear at the end of a mission. However, the efficacy of these measures is still under discussion. In the recent years, a greater awareness of the threat posed by space debris to the future access to space is emerging and initiatives such as ESA Clean Space actively promote the idea of a sustainable use of space. From this point of view, the guidelines for space debris mitigation may take inspiration from the ones developed to create a more sustainable use of resources on Earth to limit global warming.

Among different indicators that have been developed to measure the sustainability of our way of life (e.g. CO<sub>2</sub> footprint), the labelling of large household appliances appears to be a successful example, able to shift the market towards more efficient and more environmental friendly products. The European energy label (Figure 1) was introduced in 1994 for cold appliances (e.g. freezers, refrigerators), and then extended in the following years to washing machines and dishwasher [12]. In the years since its adoption, the seven-level coloured scale has become a well known indicator of energy efficiency, applied (unofficially) also to cars, buildings, and planes.

The labelling of appliances was introduced to fill the so-called *energy-efficiency* gap [2], i.e. the fact that consumers were not aware of the consumption of their appliances. This had a direct impact both on the *private* level in terms of the cost of bills, and on the *society* level in terms of the energy demand and the environmental consequences. The eco-labelling contributed to orient the market towards more efficient products, with an increase of the market share of A-level appliances [2, 14]. It also helped to define a required minimum level of efficiency, for example with the ban of new refrigerators with classes D to G [12]. Finally, it contributed to create awareness in consumers and producers, so that now energy efficiency is among the drivers in the choice of a product [14]. Similarly to [11], this work analyses how the labelling approach could be applied to tackle the space debris issue. The task

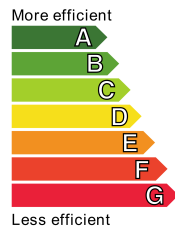


**Fig. 1** Example of energy label.

<sup>1</sup> [http://www.esa.int/Our\\_Activities/Operations/Space\\_Debris/About\\_space\\_debris](http://www.esa.int/Our_Activities/Operations/Space_Debris/About_space_debris), last access 15/06/2016

to define a *debris label* for spacecraft should start from the analysis of the main differences with respect to the case of household appliances. The first important difference is that the labels for appliances are targeted to the final users to orient their decision while buying. For satellites this approach is not feasible as currently missions are developed *ad-hoc* to provide specific data and services. For this reason, labelling a spacecraft should address mostly the spacecraft operators, for example with respect to their interface with space agencies and external organisations.

Connected to this point, it should be observed that the *private* cost of operating a spacecraft with a high *debris index* is less direct than the case of bills for a household. For example, putting spacecraft in a congested orbit could increase the operational cost due to the need of performing more collision avoidance manoeuvres. On the other hand, the decision to dispose a spacecraft at the end of its mission may not bring a direct economic benefit to its operator. This observation suggests that a *debris label* would make sense only if implemented within processes such as licensing of the spacecraft before the launch, insurance, or provision of collision avoidance services by external providers.

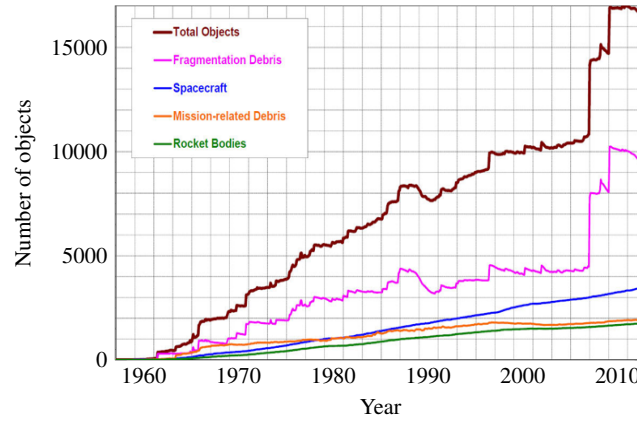


**Fig. 2** Growth of the catalogued population of objects in Earth orbit [3].

Another important decision to make for such an index is what should be measured. It was observed that the long term evolution of the space debris environment is highly affected by the fragmentation of large intact objects. Figure 2 shows the evolution of the number of objects in orbit with time and one can observe the effect of the fragmentation of Fengyun-1C and of the Iridium-Cosmos collision. A fragmentation can be caused by explosion (for example due to a failure on-board) or by a collision with another object. In both cases, a cloud of fragments is generated: the cloud, initially dense and localised, spreads under the effect of different forces, so that a fragmentation is able to affect objects in different orbital regimes.

A way to measure the severity of the consequences of these fragmentation is to look at the increase in the collision risk for operational satellites. It is very impor-

tant to underline that this is only one possible option; alternative approaches may be based on the analysis of the fragments still in orbit after a certain time period or the increase in the collision risk for the whole population (so considering not only operational satellites, but also spent satellites and rocket bodies) [5, 13]. The reason why this work suggests to look at the effects on operational satellites is because this can be more easily connected to the cost to operators due to fragmentations (*private* cost). For example, a recent analysis by ESA Space Debris Office [6] has shown how the fragmentation of Fengyun-1C and the Iridium-Cosmos collision have affected the number of conjunctions and collision avoidance manoeuvres for some ESA missions. In addition, the collision risk for operational satellites may also be seen as an indicator of the availability of future access to space (*shared* cost) because the orbital regions with most operational satellites are the ones that offers a privileged point of view for Earth observation. For example, this is the case of sun-synchronous orbits, which allows the Earth to be observed with constant illumination conditions. Therefore, they are expected to be an important asset also in the future.

For these reasons, the proposed index is based on the evaluation of the consequences of fragmentations on operational satellites. In addition, the likelihood of these fragmentations to happen should be considered. For explosions, the probability can be estimated starting from historical data on fragmentations in orbit, whereas the probability of collisions depends on the orbital region where the spacecraft operates. In summary, the index will have the following structure

$$\text{Index} = p_e \cdot e_e + p_c \cdot e_c \quad (1)$$

where  $p_e$  is the probability of an explosion happening,  $e_e$  measures the effects of the explosion on operational satellites,  $p_c$  is the probability of a collision happening, and  $e_c$  measures the effects of the collision on operational satellites. The term  $e_c$  was already developed [9], so this work will focus on the explanation of the other three terms.

## 2 Method

To assess the effect on operational satellites, a set of representative targets is defined. This is done to avoid having to propagate the trajectories of all operational spacecraft and to build a reference set that is robust to the variation of some elements in the population. In this way, there is no need to regenerate the results after each new launch. A way to define this representative set is to look at the distribution the cross-sectional area of operational satellites in semi-major axis and inclination. A grid in these two dimensions is introduced and, for the cells where most targets are concentrated, a representative target is defined, with mass and area equal to the average values among the object in the cell, and orbital parameters equal to centre of the cell.

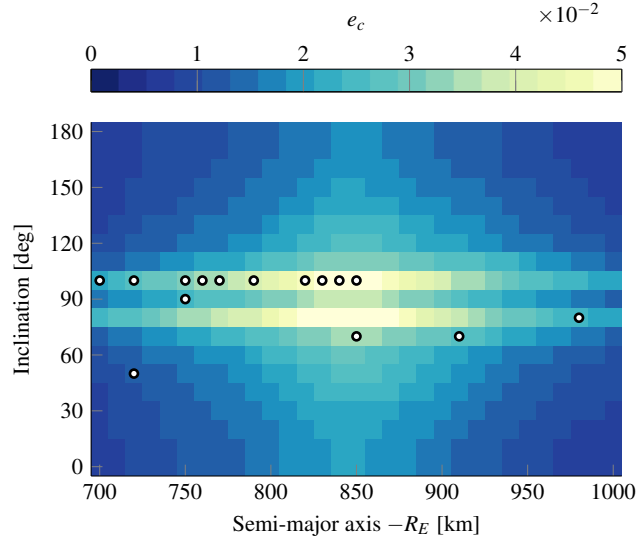


**Fig. 3** Reference map: variation of the term  $e_c$  with the orbital parameters [9].

Once the target set is defined, the effect of fragmentations can be evaluated. A key point of the suggested approach is not to compute the index only for specific objects, but rather to study its dependence on parameters such as orbit altitude, inclination, and the spacecraft mass. The same grid in semi-major axis and inclination is now used to defined possible orbits where the fragmentations occurs. Figure 3 shows the variation of the component  $e_c$  of the index obtained in [9], computed as

$$e_c = \sum_{j=1}^{N_T} w_j p_{c,j}, \quad (2)$$

where  $p_{c,j}$  is the cumulative collision probability for each representative target and  $w_j$  a weighting factor to consider that each representative target represents a different share of the total area distribution. The grey markers refer to the representative targets identified with the approach based on the cross-sectional area.

One of the advantages of studying the index dependence on these parameters (rather than only evaluating single spacecraft) is that maps such as Figure 3 clearly show which are the most critical orbits. Observe also that Figure 3 was obtained simulating always the same fragmentation and changing only its location; in particular, the mass involved in the fragmentation is fixed. It can be shown that if the fragmenting mass is changed, the value of the index changes accordingly following a power law [9]. This follows directly from the equations of the breakup model used to generate the fragments. This behaviour is particularly convenient because it means that no additional simulations are required if one wants to obtain the same map as in Figure 3 for a different value of the fragmenting mass; it is sufficient to rescale the result already obtained.

In this way, only the reference map in Figure 3 is needed to compute  $e_c$  for any specific spacecraft. This requires to rescale the reference map to the value of the mass of the studied object that we want to evaluate and to interpolate the reference map to find the value of the index for its specific orbital parameters. This means that the process of computation of the index is split into two parts: the generation of the reference map and the actual computation of the index. The generation of the map requires operations that are computationally expensive and that rely heavily on the availability of efficient methods for debris cloud propagation [8] and computational resources. Once the reference map is generated, this can be saved and stored. When the index needs to be computed for some specific objects, this can be done by simply rescaling and interpolating, as explained in the previous paragraph. These operations are fast and can be easily implemented in different programming languages.

Following this approach, the index can be computed in a matter of seconds for all the objects in a database. This is important because it could be expected that the index may be computed also outside research organisations, for example in companies and institutions with no access to the propagation methods and the computational resources required by the generation of the reference map. This rationale is kept also in the development of the new terms.

## 2.1 Effect of explosions

For the case of the effect of explosions ( $e_e$ ), a similar approach to the one previously described can be adopted. Explosions tend to produce larger fragments with lower speed compared to collisions, so different equations are used for the generation of the fragments. In addition, in the NASA breakup model [4], the mass of the exploding spacecraft does not appear explicitly (differently from the case of collisions). In particular, the number of fragments generated by an explosion with size equal or larger than  $L_c$  is given by

$$N(L_c) = 6SL_c^{-1.6}, \quad (3)$$

where  $L_c$  is in m and  $S$  is type-dependent unitless number that acts as a scaling factor for the explosions. The initial version of the breakup model uses only  $S = 1$ , but a later update to the model suggests that its value can change between 0.1 and 1, depending on the explosion type [7]. The parameter  $S$  can be used to introduce a dependence on the mass in Equation 3. First, one can observe that the mass of generated fragments depends linearly on  $S$ ; keeping the constraint  $S \leq 1$ , the maximum fragment mass is around 160 kg. Following the observation that explosions usually involved only specific components and not the whole space objects, the following relationship for  $S$  was found

$$S = \begin{cases} k \frac{m_{\text{obj}} [\text{kg}]}{10000 [\text{kg}]}, & \text{for } km_{\text{obj}} < 10000 \text{ kg} \\ 1 & \text{for } km_{\text{obj}} \geq 10000 \text{ kg} \end{cases}, \quad (4)$$

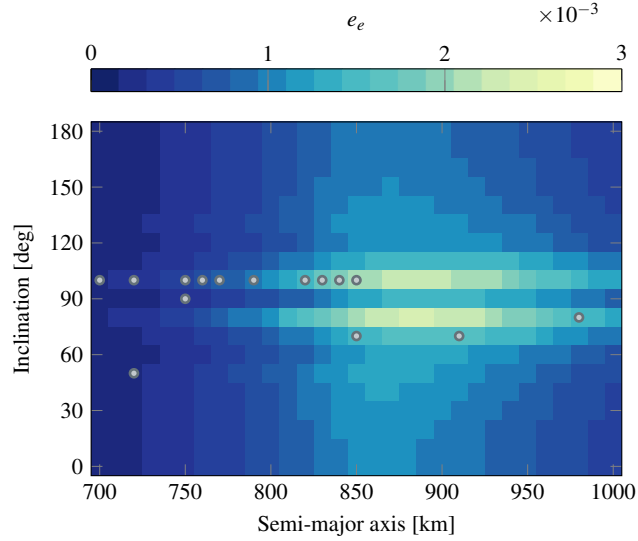


**Fig. 4** Reference map: variation of the term  $e_e$  with the orbital parameters.

with  $k = 1$  for payloads and  $k = 9$  for rocket bodies. The different value of  $k$  for payloads and rocket bodies derives from the analysis on the number of fragments produced per kg for the two classes of objects according to the data available in DISCOS<sup>2</sup> (Database and Information System Characterising Objects in Space). More details on this can be found in [10].

Following the same approach used for  $e_c$ , also in the case of explosions different fragmentations were simulated changing the orbital parameters of the orbit where the breakup occurs, while keeping constant the value of the mass of the fragmenting objects. The effect was measured on the same representative targets to assess their sensitivity to the breakup conditions. Figure 4 shows the result of this analysis by visualising the value of  $e_e$  obtained, similarly to the case of collisions, as

$$e_e = \sum_{j=1}^{N_r} w_j p_{c,j}, \quad (5)$$

where  $p_{c,j}$  is the cumulative collision probability for each representative target due to the fragments generated by the explosions and  $w_j$  the weighting factors defined in Equation 2. Similarly to the results in Figure 3, one can observe the role of the inclination with two horizontal bands that correspond to fragmentations where the targets will cross the resulting fragment cloud in the latitude regions with the maximum fragment density. Compared to the case of the collisions in Figure 3, the dependence on the altitude is more localised for the case of explosions.

<sup>2</sup> <https://discosweb.esoc.esa.int>

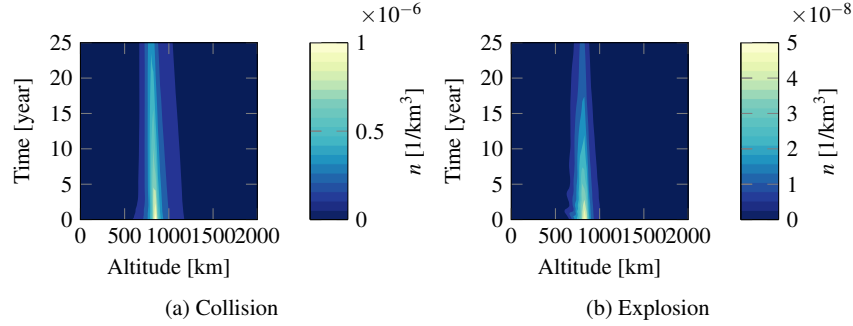


**Fig. 5** Evolution of the density profile with time for two fragmentations starting at 850 km of altitude.

This is due to the fact that, as already mentioned, explosions and collisions produce fragments with different characteristics. In particular, the fragments generated by explosions have a lower variation in velocity, so they remain more concentrated around the orbit where the fragmentation occurred.

The behaviour can be visualised by studying the persistence of the fragments in orbit, for the two cases, as shown in Figure 5 that represents the evolution of the cloud density profile with time for a collision and an explosion starting from an orbit with altitude equal to 850 km. In the case of the collision, the complete fragmentation of a satellite of 10000 kg is simulated, whereas for the explosion the maximum fragment mass is equal to 160 kg and this explains the difference in the order of magnitude for the density. Also from this representation, one can notice how the explosion appears to affect a smaller range of altitudes and the corresponding cloud to decay quicker than the one generated by the collision.

## 2.2 Probability of collision

The probability of a collision happening ( $p_c$ ) can be estimated by using the analogy with the kinetic theory of gas, so that the cumulative collision probability is written as

$$p_c = 1 - \exp(-\rho \Delta v A_c \Delta t), \quad (6)$$

where  $\rho$  is the debris density at the spacecraft altitude,  $\Delta v$  is the collision velocity,  $A_c$  the cross-sectional area, and  $\Delta t$  is the time.

As only catastrophic collisions are considered, the value of  $\rho$  depends on the mass of the studied object. For this reason,  $\rho$  should express the density of objects able to trigger a catastrophic collision. This means that, given the mass of the object, the energy threshold for catastrophic collisions (40 kJ/g) should be applied to find the limit on the impactor size. Then, the corresponding density is derived from the



ESA tool MASTER (Meteoroid and Space Debris Terrestrial Environment Reference).

For the relative velocity, MASTER is used again to identify the most likely impact velocity given the orbital parameters of the studied object. An example of this analysis is shown in Figure 6 for an orbit at 814 km of altitude and  $98^\circ$  of inclination. The distribution can be used to associate to each orbital configuration, the most likely impact velocity. For example, in Figure 6 the peak is at  $\Delta v = 14.5$  km/s; alternatively, the reference impact velocity can be found by computing the integral mean of the distribution and in this case  $\Delta v = 13.6$  km/s is obtained. This second option is the one used in the following. This process was repeated on a set of reference orbits, using the same grid as in Figure 3, so with a spacing of 10 km in semi-major axis and  $10^\circ$  in inclination. The eccentricity is put equal to zero for all the cases; in addition, no variation in the other parameters (i.e. the longitude of the ascending node  $\Omega$  and the argument of periapsis  $\omega$ ) is considered as it is assumed that the background population is uniformly distributed with respect to these parameters.

Also the terms used to build  $p_c$  can be precomputed and interpolated, so that the analysis of the collision risk can be quickly performed on all the objects in a database. For example, Figure 7 shows the ten payloads with the highest value of the collision risk ( $I_c = p_c \cdot e_c$ ) among the objects in the the ESA DISCOS database and in orbit between 700 and 1000 km. One can observe how with  $I_c$  is considered instead of only  $e_c$  as in [9], all the top objects belong to the peak areas with at altitudes between 760 and 870 km. In particular, Cosmos 2502 and 2455, both in an orbit at 905 km of altitude, were in the top ten objects when only  $e_c$  is considered, but their relative criticality is reduced when also  $p_c$  is considered because that orbital region is less critical in terms of background debris population. Similarly for Cosmos 2486 and 2441, in orbit at 720 km of altitude, that are in the top ten when only the effects

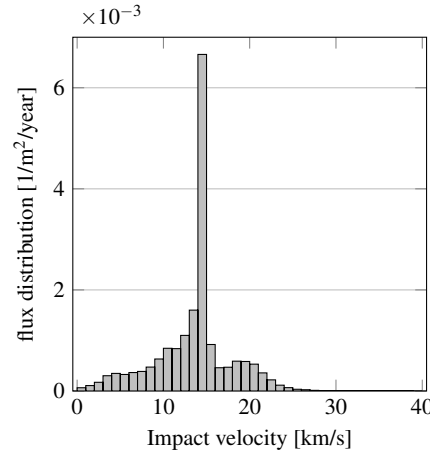


**Fig. 6** Impact velocity distribution obtained with MASTER for an orbit at 814 km of altitude and  $98^\circ$  of inclination.

of a fragmentation are considered, but ranks over the 120th place when also the collision probability is taken into account. The first object is the same (Envisat) for both classifications (i.e. only  $e_c$  or  $I_c$ ).

### 2.3 Probability of explosion

The estimation of the probability of explosion is performed starting the data on historical fragmentations available on ESA DISCOS. First, the data in DISCOS was analysed by looking at the classification of all events based on the cause of fragmentation. Figure 8 shows the frequency of fragmentation causes for payload and rocket bodies: as expected, the distribution is different for two classes and this should be reflected in the estimation of the  $p_e$  term should take into consideration this classification. In addition, the probability of explosion should take into account only events due to propulsion failures, battery failures or unknown fragmentation cause. The events due to collisions or deliberate destruction are not relevant to the development of a model of the explosion probability, whereas fragmentations due to atmospheric forces or attitude failures cannot be modelled with the breakup model used for the term  $e_e$ . In addition, only fragmentations occurred in Low Earth Orbit (LEO) will be considered in the following.

The statistical modelling of the term  $p_e$  was built by looking at fragmentations occurred in LEO, involving objects launched after 1985 and distinguishing between payloads and rocket bodies. The adopted approach is the following: for each class of

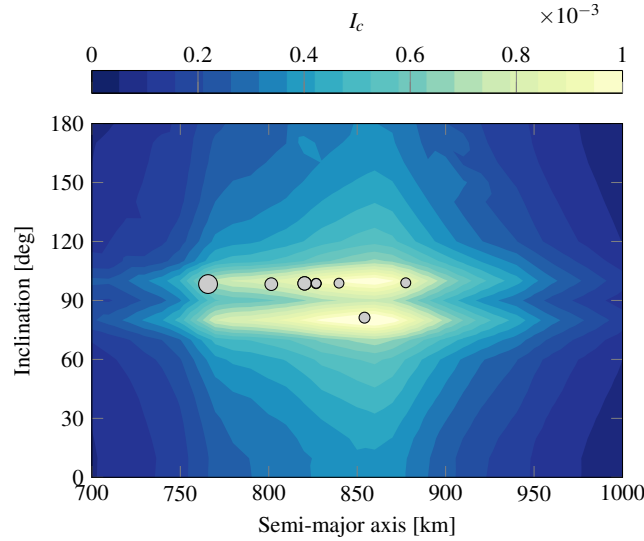
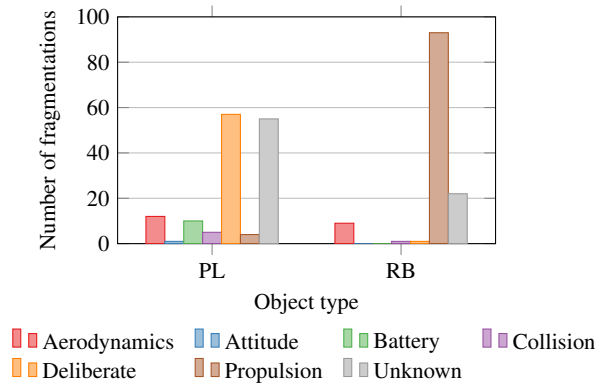


**Fig. 7** Top ten payloads with the highest value of  $I_c = p_e \cdot e_c$ .

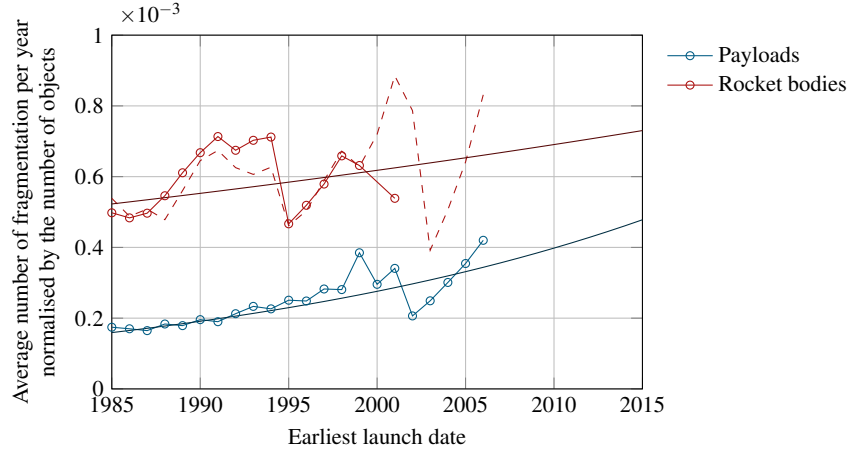
objects (i.e. payloads and rocket bodies), the number of fragmentations in a year is registered and it is assumed that it can be described with a Poisson distribution. The chi-squared test is used to verify if this hypothesis is acceptable. If so, the parameter of the Poisson distribution gives the estimated average number of fragmentation in a year. In order to obtain a value that can be inserted in Equation 1, the average number of fragmentations per year needs to be normalised with the number of launched objects.

Figure 9 shows the value of the average number of fragmentations normalised with the number of objects considering the fragmentations and the launched objects in LEO after a certain epoch. The choice to define a value of explosion probability for all the objects launched after a certain date instead of defining a value for each year or each decade is due to the fact that the latter approach leads to subsets with few samples where the chi-squared test is not conclusive and, more in general, the number of events is too low to obtain robust statistics. Already in the years after 2006, the average number of fragmentations in a year cannot be found because the total number of events is too low to apply the chi-squared test. In addition, in the years 2000 and 2002-2006 the estimation for the rocket bodies fail. For this reason, the value is estimated using the Poisson approximation for all the events (rocket bodies and payloads) and subtracting the value obtained from the payloads. In this way, the dashed curve in Figure 9 is obtained.

One can observe how rocket bodies have a larger probability of explosion than spacecraft. In addition, the increasing trend in the curve means that when considering more and more recent objects, the number of objects is reduced, but the number of fragmentations decreases at a lower rate. This is consistent with the observed trend of fragmentations with the launch year of the objects (Figure 10). In addition, one can observe how the peaks of fragmentations for objects launched in 2002 and 2006 is reflected in the change of the slope of the curve in Figure 9. These curves can be, in a first step, approximated with an exponential function as shown in Figure



**Fig. 8** Classification of past fragmentations involving payloads (PL) and rocket bodies (RB).



**Fig. 9** Average number of fragmentations per year normalised by the number of objects.

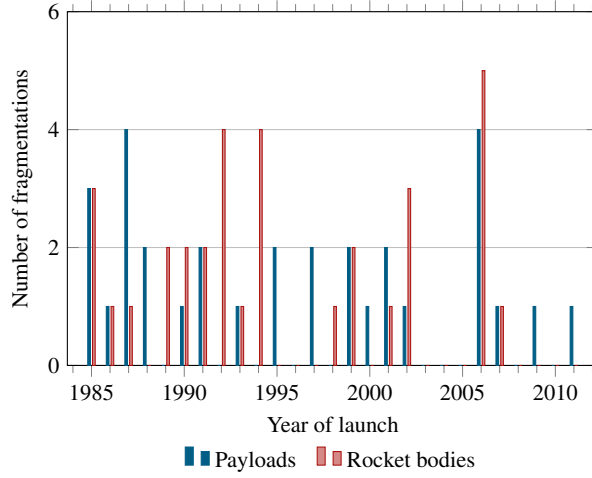


**Fig. 10** Distribution of fragmentation events in LEO as a function of the year of launch. The numbers refer only to events due to battery or propulsion failures and with unknown fragmentation cause.

9. To limit the risk associated to extrapolation, the exponential function is used only up to the present epoch and then this value is applied for all the future launches.

In summary,

$$p_e = \begin{cases} 0 & \text{for } y_L < 1985 \\ \alpha \exp[\beta(y_L - 1985)] & \text{for } 1985 \leq y_L \leq 2016 \\ \alpha \exp[\beta(2016 - 1985)] & \text{for } y_L > 2016 \end{cases}, \quad (7)$$

**Table 1** Fitting parameters for the probability of explosion

Parameter	Payload	Rocket bodies
$\alpha$	1.59193E-04	5.22821E-04
$\beta$	3.66550E-02	1.11388E-02

where  $\alpha$  and  $\beta$  are the fitting parameters reported in Table 1. It is important to observe how the expression for  $p_e$  in Equation 7 introduces a temporal dependence, so that, in accordance to historical data, objects launched more recently present a *higher* probability of explosion. Another way to explain the ascending trend of  $p_e$  with time is that, as shown in Figure 10, the number of explosions per year of launch does not improve in recent years. So while the average number of fragmentations per year is quite stable, moving along the  $x$ -axis in Figure 9 a smaller and smaller subset of space object is considered, hence the ascending trend.

### 3 Eco-labelling of space missions

Now that all the four terms have been defined, the debris index can be computed for any space objects in the altitude range of 700-1000 km. The expected output of the proposed debris index is to have a metric able to distinguish space missions on the basis of two main aspects: the mass of the spacecraft and the orbital regime where the spacecraft will operate. Current work is undergoing to take into consideration also the implementation of end-of-life disposal strategies.

The numerical value of this metric would depend on the distribution of operational satellites used to evaluate the effect of a fragmentation, so a process of normalisation is suggested. Only in this way metrics computed in different times (with a different underlying population of operational satellites) are comparable. This would also facilitate the interpretation of the numerical value of this debris index.

**Table 2** Definition of severity categories [1] and possible meaning for the description of the consequences of a breakup.

Severity	Dependability effects	Safety effects	Breakup consequences	Symbol
Catastrophic	Failure propagation	Severe detrimental environmental effects	Subsequent collisions	■
Critical	Loss of mission	Major detrimental environmental effects	Major increase in collision risk	■
Major	Major mission degradation		Increase in collision avoidance manoeuvres	■
Minor	Minor mission degradation		Negligible	■

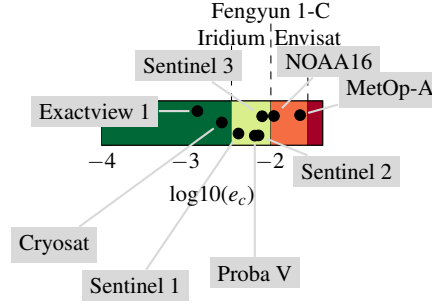


**Fig. 11** Example of fragmentation severity classification for some representative missions.

An attempt in this direction was already performed for the classification of the effect of a collision (term  $e_c$ ). In that case, some severity levels (Table 2) were derived from the FMECA (Failure Modes, Effects, and Criticality Analysis) applied during the quality assessment of space missions. The transition between two levels was marked by reference fragmentations.

Figure 11 shows the classification applied to several missions and, as expected, large missions in sun-synchronous orbits (e.g. Sentinel 3) have larger value of  $e_c$  than small missions (e.g. Exactview). A similar approach could be adopted also for the whole index as defined in Equation 1. The most challenging aspect of the process would be to define levels and reference scenarios to build a scale that enables an immediate understanding as in the case of the labelling of household appliances.

A classification of the effects on the space debris environment of a mission is going to be accepted only if all the relevant stake holders are involved in its definition (especially in the formulation of the reference scenarios and the corresponding criticality levels). This means that agencies, operators, manufacturers, and users should be involved in the process. Only in this way it can be avoided that such a classification appears to *blame* specific players.

In addition, such classification should be associated also to a *positive* message. For example, agencies may consider to implement a lean licensing process for *A-level* spacecraft. This would be interesting in particular for small satellites missions that would see a benefit in be more compliant with the guidelines, while now some operators may be tempted to launch their small satellites in a crowded orbital region just because a cheap launch opportunity is available. Similar advantages may be envisioned also in terms of insurance of cost of collision avoidance services provided by external companies. All these measures would enhance the *private* interest of satellite operators to adopt the proposed classification and avoid that it exists only for communication purposes.

## 4 Conclusions

This work described a possible formulation for a debris index, that is a metric for the impact of a space object (i.e. spacecraft or rocket body) on the space debris environment. The index is a development of a previous formulation that looked at how the potential fragmentation of the studied object would affect the collision probability for operational satellites. In the current work, this idea is expanded by considering the probability of these fragmentation happening, distinguishing between collisions and explosions. When assessing the effects of collisions and explosions it was observed how the latter tend to have a more localised effect. It was shown how this is related to the fact that, according to employed breakup model, explosions produce larger fragments with a lower velocity variation compared to collisions. For what concerns the probability of collision, it was estimated using the analogy with the kinetic theory of gases. ESA MASTER was used to retrieve the density of debris objects at different altitudes and the most likely impact velocity for different orbital regimes (defined in terms of semi-major axis and inclination). Finally, the probability of explosion was estimated starting from the data available in Discos on past fragmentations. Only events occurred in LEO after 1985 were considered; in addition, only fragmentations due to propulsion failures, battery failures or unknown cause were analysed. Applying the distinction between spacecraft and rocket bodies, a Poisson distribution is used to approximate the distribution of the number of fragmentation in a year and the resulting average value. This number is then divided by the number of objects launched in the considered time period to estimate a value of probability. By repeating this procedure for different epochs of launch, it is possible to obtain an estimation of the probability term that depends not only on the type, but also on how long the object has been in orbit. By putting together the four terms one can obtain a more complete representation of the fragmentation risk associated to a space object and, therefore, to its exposure and potential contribution to the space debris population. Future work will further enhance this representation by addressing the distinction among objects with different disposal strategies, the application to constellations and the extension of the applicability region of the index to the whole LEO. Finally, a possible normalisation of the index was proposed based on the definition of four levels of severity and the definition of some reference fragmentations. For the moment the definition of the levels considers only the term related to the effects of the potential fragmentation of the studied object, but the same procedure can be applied also to the complete formulation of the index. Future work will analyse the definition of meaningful reference threshold when all the terms of the index are considered.

**Acknowledgements** Francesca Letizia acknowledges the support from the EPSRC Doctoral Training Partnership at the University of Southampton, grant EP/M508147/1. Francesca Letizia thanks ESA Space Debris Office for the support received during her visiting period in ESOC where part of this work was developed. The authors acknowledge the use of the IRIDIS High Performance Computing Facility, and associated support services at the University of Southampton,

in the completion of this work. Data supporting this study are openly available from the University of Southampton repository at <http://doi.org/10.5258/SOTON/405121>

## References

- [1] European Cooperation for Space Standardisation (2009) Space product assurance: Failure modes, effects (and criticality) analysis (FMEA/FMECA). Tech. Rep. ECSS-Q-ST-30-02C, ESA Requirements and Standards Division
- [2] Heinzle SL, Wüstenhagen R (2012) Dynamic adjustment of eco-labeling schemes and consumer choice the revision of the eu energy label as a missed opportunity? *Business Strategy and the Environment* 21(1):60–70, DOI 10.1002/bse.722
- [3] IADC Steering Group (2013) Space Debris. IADC Assessment Report for 2011
- [4] Johnson NL, Krisko PH (2001) NASA's new breakup model of EVOLVE 4.0. *Advances in Space Research* 28(9):1377–1384, DOI 10.1016/S0273-1177(01)00423-9
- [5] Kebschull C, Radtke J, Krag H (2014) Deriving a priority list based on the environmental criticality. In: 65th International Astronautical Congress, International Astronautical Federation, iAC-14.A6.P48
- [6] Krag H, Merz K, Flohrer T, Lemmens S, Bastida Virgili B, Funke Q, Braun V (2016) ESAs Modernised Collision Avoidance Service. In: 14th International Conference on Space Operations
- [7] Krisko PH (2011) Proper Implementation of the 1998 NASA Breakup Model. *Orbital Debris Quarterly News* 15(4):1–10
- [8] Letizia F, Colombo C, Lewis HG (2015) Multidimensional extension of the continuity equation method for debris clouds evolution. *Advances in Space Research* 57(8):624–1640, DOI 10.1016/j.asr.2015.11.035
- [9] Letizia F, Colombo C, Lewis HG, Krag H (2016) Assessment of breakup severity on operational satellites. *Advances in Space Research* 58(7):1255 – 1274, DOI 10.1016/j.asr.2016.05.036
- [10] Letizia F, Colombo C, Lewis HG, Krag H (2017) Fragmentation risk as a metric of the impact on the space debris environment. (Submitted for publication)
- [11] Lewis HG, George SG, Schwarz BS, Stokes H (2013) Space debris environment impact rating system. In: Ouwehand L (ed) Sixth European Conference on Space Debris, ESA Communications
- [12] Mills B, Schleich J (2010) What's driving energy efficient appliance label awareness and purchase propensity? *Energy Policy* 38(2):814–825
- [13] Rossi A, Valsecchi GB, Alessi EM (2015) The Criticality of Spacecraft Index. *Advances in Space Research* 56(3), DOI 10.1016/j.asr.2015.02.027
- [14] Sammer K, Wüstenhagen R (2006) The influence of eco-labelling on consumer behaviour results of a discrete choice analysis for washing machines. *Business Strategy and the Environment* 15(3):185–199, DOI 10.1002/bse.522